# Field-tuned Fermi liquid in quantum critical $YFe_2Al_{10}$

K. Park,[1] L. S. Wu,[1,2] Y. Janssen,[1] M. S. Kim,[1,2] C. Marques,[2] and M. C. Aronson[1,2,*]

[1]*Brookhaven National Laboratory, Upton, New York 11973, USA*

[2]*Department of Physics and Astronomy, Stony Brook University, Stony Brook, New York 11794, USA*

(Received 19 August 2011; published 20 September 2011)

We present measurements of the magnetization $M$, ac susceptibility $\chi'$, electrical resistivity $\rho$, and specific heat $C$ in single crystals of metallic $YFe_2Al_{10}$. The magnetic susceptibility follows a Curie-Weiss temperature dependence for 75 K $\leqslant T \leqslant$ 750 K, with a fluctuating Fe moment of $0.45\mu_B$/Fe, and the ac susceptibility $\chi'$ diverges at lower temperatures $\chi' \sim T^{-1.28\pm0.04}$ when the ac field is in the basal plane. The field $B$ and temperature $T$ dependencies of the magnetization $M$ are well described by the scaling expression $MT^{-\beta} = \mathcal{F}(B/T^{\beta+\gamma})$ for 1.8 K $\leqslant T \leqslant$ 30 K and for fields larger than $0.1T$. These results indicate that strong quasi-two-dimensional critical fluctuations are present that can be suppressed by magnetic fields. The magnetic and electronic parts of the specific heat $C_M$ show a similar divergence for 0.4 K $\leqslant T \leqslant$ 12 K, where $C_M/T \sim T^{-0.47\pm0.03}$. The divergences in $\chi'$ and $C_M/T$ indicate that $YFe_2Al_{10}$ is located near a quantum critical point, and no magnetic order is observed above 0.09 K. We argue that our results are inconsistent with quantum impurity or disorder models, suggesting instead that $YFe_2Al_{10}$ is on the verge of bulk magnetic ordering, and that the critical fluctuations that are associated with this quantum critical point lead to the divergencies in $C_M/T$ and $\chi'$.

DOI: 10.1103/PhysRevB.84.094425 PACS number(s): 64.70.Tg, 71.10.Hf, 75.30.Kz

## I. INTRODUCTION

There is mounting evidence that quantum critical points (QCPs) where magnetic order vanishes are central to the phase diagrams of the doped cuprates,[1–3] iron pnictides,[4] heavy-electron compounds,[5–7] and low-dimensional conductors.[8] Novel critical phenomena are observed near these $T = 0$ phase transitions.[9–11] The coupling of these critical modes to the electronic structure may lead to electronic delocalization transitions,[12,13] and ultimately to exotic electronic phases such as unconventional superconductivity[14,15] and to partially ordered "spin-nematic" states.[16,17]

To what extent are these QC properties truly universal, requiring only a metallic system where magnetic order is driven to instability by pressure, magnetic field, or compositional variation?[18] Pressure and magnetic field tuning experiments on the $f$-electron-based heavy-electron compounds have so far provided us with the most detailed information about this process.[5–7] Here, the magnetic order is replaced at the QCP by a strongly interacting Fermi liquid (FL) that expands into a broader range of temperatures as the system is tuned further into the paramagnetic state. In some cases the quasiparticle mass diverges at or near the QCP, and this breakdown of the FL description can be associated with a $T = 0$ transition between the magnetically ordered state where the $f$ electron is localized, and the paramagnetic (PM) state where it is delocalized and absorbed in the Fermi surface (FS).[19–23]

By comparison, the description of QC behavior is much more limited in systems where magnetism is derived from the $d$ electrons. It is well established that pressure or field can drive magnetic ordering to $T = 0$, via a first- or second-order transition.[24–28] Other compounds have singular temperature dependencies in specific heat and magnetic susceptibility[29–35] that signal their proximity to a QCP, although the use of doping to approach the QCP can replace the intrinsic critical fluctuations with mean-field behavior.[27,36,37] Competing orders such as superconductivity in the cuprates[38] and the spin-nematic phase in $Sr_3Ru_2O_7$ (Ref. 16) have masked much of their experimental phase space, making a clear demonstration of quantum critical behavior challenging. For these reasons, there is much interest in identifying new stoichiometric compounds whose magnetism is derived entirely from $d$ electrons, and where magnetic order can be readily tuned to a QCP.[18]

We report measurements on single crystals of $YFe_2Al_{10}$, which is a chemically ordered and stoichiometric compound.[39] Previous experiments on polycrystalline samples reported power-law increases in the specific heat $C/T$ and the dc susceptibility $\chi$,[40] and our measurements are focused on exploring the critical phenomena associated with the low-temperature susceptibility, magnetization, and specific heat. Since there is no sign of magnetic order at temperatures as low as 0.09 K, these measurements indicate that $YFe_2Al_{10}$ is located very near a QCP, without the need for fine tuning by a control variable such as composition or pressure.

## II. EXPERIMENTAL DETAILS

We synthesized faceted and platelike single crystals of the compounds $YT_2Al_{10}$ ($T$ = Fe,Ru,Os) with typical dimensions of ≈1 cm from stoichiometric quantities of $T$ and Y in an aluminum flux. We used WINGX[41] to refine our single-crystal x-ray-diffraction patterns, and to confirm previous reports[39] that $YFe_2Al_{10}$ forms in an orthorhombic stacking variant of the tetragonal $ThMn_{12}$ structure, where the fourfold ac planes are stacked along the $b$ axis. We obtained a refinement factor $R1 = 0.0164$, permitting no more than 1% variation in site occupancy, ruling out the considerable Fe/Al site interchange characteristic of the Fe-rich members of the $YFe_xAl_{12-x}$ family.[42]

## III. MAGNETIC MEASUREMENTS

The intrinsically magnetic character of $YFe_2Al_{10}$ is evident from measurements of the temperature-dependent magnetic susceptibility, obtained using a Quantum Design Magnetic Property Measurement System. Figure 1(a) shows the ac

 

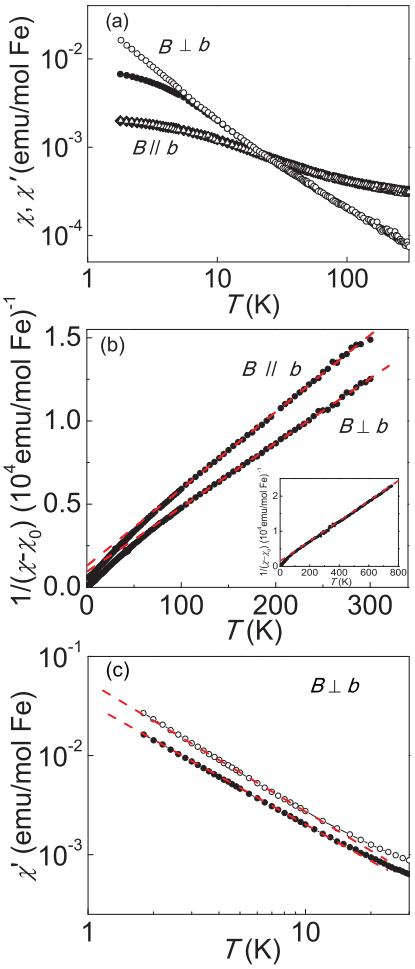


FIG. 1. (Color online) (a) Temperature dependencies of dc susceptibility $\chi$(•) and ac susceptibility $\chi'$ (○), where the dc field $B = 1$ T and the ac field $B' = 0.4$ mT are applied both parallel and perpendicular to the $b$ axis, as indicated. (b) The inverse of the temperature-dependent parts of the dc susceptibility $(\chi - \chi_0)$ display Curie-law temperature dependencies (red dashed lines) for $B \perp b$ and $B \parallel b$. The inset shows that the Curie law extends up to 750 K in a crystal with indefinite orientation. (c) The ac susceptibility $\chi'$ follows a power-law temperature dependence for $T \leqslant 20$ K. The power laws are indicated by red dashed lines, yielding exponents that are similar in two different samples taken from different batches (sample 1: •, slope $= 1.22 \pm 0.03$; sample 2: ○, slope $= 1.33 \pm 0.03$). The small differences in the magnitudes of $\chi'$ of the two samples are likely the result of small inaccuracies in aligning the crystalline axes relative to the magnetic field.

susceptibility $\chi'$, measured in an ac field $B' = 0.4$ mT, and the dc susceptibility $\chi = M/B$, where the magnetization $M$ is divided by the 1 T dc measuring field $B$. For temperatures $T \geqslant 30$ K, $\chi$ and $\chi'$ obey similar Curie-law temperature dependencies $\chi = \chi_0 + C/(T - \theta)$ that extend to temperatures as high as 750 K. The Curie constants give fluctuating moments with magnitudes $0.41\mu_B$/Fe ($B \parallel b$) and $0.45\mu_B$/Fe ($B \perp b$), and Weiss constants of $-28$ K ($B \parallel b$) and $-24$ K ($B \perp b$) [Fig. 1(b)]. The temperature-independent background $\chi_0$ is $2.5 \times 10^{-4}$ emu/mol for $B \parallel b$, ≈100 times larger than for $B \perp b$ [Fig. 1(a)]. The fluctuating moments responsible for the Curie law are much reduced from expected Hund's rule values, but vary only by ≈25% among crystals taken from different batches. The small but negative value for $\theta$ indicates a net ferromagnetic Weiss field, although there is no sign of magnetic order in the susceptibility data above 1.8 K.

Figure 1(a) shows that $\chi$ and $\chi'$ depend strongly on both the magnitude and direction of the measuring field at the lowest temperatures. A strong easy-plane anisotropy develops with decreasing temperature, and Fig. 1(a) shows that this anisotropy $\chi'(B' \perp b)/\chi'(B' \| b) \simeq 10$ at 1.8 K and $B' = 0.4$ mT. The fourfold anisotropy in the ac plane remains no more than a few percent in fields as large as 1 T. $\chi'$ continues to increase with decreasing temperature at the lowest temperatures when $B' \perp b$, but saturates at low temperatures in larger dc fields, or if $B' \parallel b$. For $T \leqslant 15$ K, Fig. 1(c) shows that for $B \perp b \chi'(T) \sim T^{-\gamma}$, with $\gamma = 1.22 \pm 0.03$, while in a second sample $\gamma = 1.33 \pm 0.03$, giving an average value $\gamma = 1.28 \pm 0.04$. These observations suggest that $\chi'$ is controlled by critical fluctuations residing largely in the ac plane, associated with a $T = 0$ magnetic phase transition whose criticality can be suppressed by magnetic fields.

Heavy-fermion compounds often display field and temperature scaling near QCPs,[11,43–45] and this is also true for $YFe_2Al_{10}$. The magnetization $M$ becomes increasingly nonlinear with $B \perp b$ as the temperature is reduced [Fig. 2(a)], saturating at a high field value that can vary as much as ≈25% among samples from different batches. Given the large magnetic anisotropy evident in Fig. 1(a), inaccuracies of only a few degrees in aligning crystal axes with respect to the field direction can fully explain this apparent variation in the high field magnetization found in different measurements. We have considered the possibility that the field and temperature dependencies of the magnetization are derived from those of simple paramagnetic impurities. Accordingly, we have replotted the isotherms of $M(B)$ as functions of $B/T$ in Fig. 2(b). No collapse of the data is observed, and the Brillouin

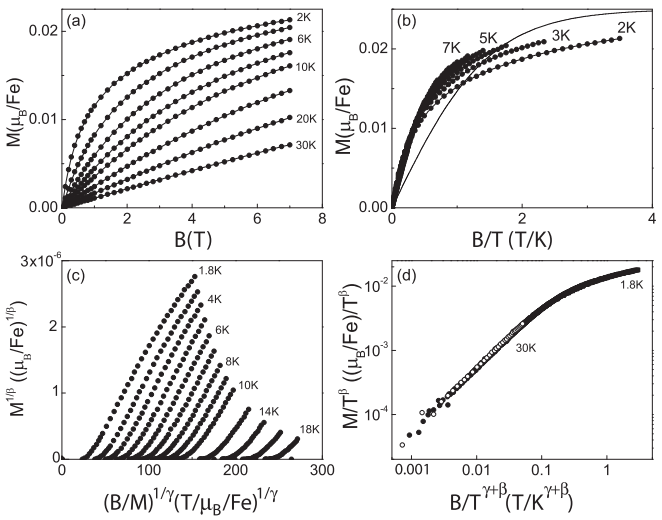


FIG. 2. (a) Magnetization $M$ as a function of field $B \perp b$, at indicated temperatures. (b) Data from (a), plotted as functions of $B/T$. Solid line is the $S = 1/2$ Brillouin function, with a scaled magnitude. (c) Modified Arrott plots of data from (a), where $\beta = 0.3$ and $\gamma = 1.2$. (d) Scaling plot for data from (a), using $\beta = 0.3$ and $\gamma = 1.2$.

function describes the data very poorly. Similarly, we point out that $M(B)$ is effectively linear in field above 30 K, suggesting that contamination from ferromagnetic Fe is not responsible for the low-temperature nonlinearities in $M(B)$.

We have carried out a modified Arrott plot analysis of $M(B,T)$ [Fig. 2(c)], where an appropriate choice of $\gamma$ and $\beta$ makes isotherms of $M^{1/\beta}$ linear and parallel functions of $(B/M)^{1/\gamma}$. Figure 2(c) shows that no spontaneous moment develops in $YFe_2Al_{10}$ above 1.8 K, and that for $T \leqslant 10$ K, $\beta = 0.3 \pm 0.05$ and $\gamma = 1.2 \pm 0.1$. Figure 2(d) demonstrates the quality of the scaling collapse of $M(B,T)T^{-\beta} = \mathcal{F}(B/T^{\gamma+\beta})$ found for temperatures $1.8\ \text{K} \leqslant T \leqslant 30$ K, and for fields $0.1\ \text{T} \leqslant B \leqslant 7$ T. The success of this scaling analysis, reproduced in a second sample, indicates that $YFe_2Al_{10}$ is located very near a QCP, with critical fluctuations that are suppressed by fields and temperatures.

## IV. SPECIFIC-HEAT MEASUREMENTS

Further evidence for these QC fluctuations comes from the low-temperature specific heat $C$ [Fig. 3(a)], which was measured for single crystals of $YFe_2Al_{10}$ and $YRu_2Al_{10}$ using a Quantum Design Physical Property Measurement System. The phonon contribution to the specific heat of $YFe_2Al_{10}$ was estimated by rescaling the temperature dependence of the measured $C/T$ of nonmagnetic but isoelectronic $YRu_2Al_{10}$ to match that of $YFe_2Al_{10}$ above 12 K, a procedure that compensates for the slightly larger Debye temperature in $YFe_2Al_{10}$, $\theta_D(YFe_2Al_{10}) = 1.03\theta_D(YRu_2Al_{10})$. By subtracting this estimated phonon contribution $C_{ph}(T)$, we have isolated the magnetic and electronic specific heat of $YFe_2Al_{10}$, $C_M = C - C_{ph}$. $C_M/T$ is approximately temperature independent for $T \geqslant 12$ K [Fig. 3(b)], indicating that here $YFe_2Al_{10}$ is a Fermi liquid with a Sommerfeld coefficient $\gamma = C_M/T \approx 9$ mJ/mol Fe K$^2$. By comparison to the Sommerfeld constant found in nonmagnetic $YRu_2Al_{10}$ ($\gamma = 3$ mJ/mol Ru K$^2$), it is evident that there is an appreciable quasiparticle mass enhancement in the Fermi-liquid state of $YFe_2Al_{10}$, $m^*/m \simeq \gamma(YFe_2Al_{10})/\gamma(YRu_2Al_{10}) \simeq 3$. $\gamma$ varies by no more than $\simeq$20% among five different $YFe_2Al_{10}$ crystals, reflecting both the uniformity among samples from different batches and the overall accuracy of the phonon subtraction procedure. The full temperature dependence of $C_M/T$ is presented in Figs. 3(c) and 3(d). $C_M/T$ departs below 12 K from the constant value $\gamma$ that marks its Fermi-liquid state, increasing monotonically below 12 K to a weak maximum at $\approx$0.09 K. It is possible that the sharp increase in $C_M/T$ at the lowest temperatures may reflect a nuclear Schottky effect associated with the Al nuclei, although further measurements are required to fully establish this possibility. We stress that there is no definitive evidence in $YFe_2Al_{10}$ for magnetic order for temperatures as low as 0.09 K. We find in two different samples that $C_M/T$ follows a power law $C_M(T) \propto T^{-\alpha}$, with $\alpha = 0.47 \pm 0.03$ for $0.4\ \text{K} \leqslant T \leqslant 12$ K. Figure 3(d) shows that $C_M/T$ is not as well described by $C_M/T \sim -\ln T/T^*$, a temperature dependence that is found in many $f$-electron systems near QCPs.[5]

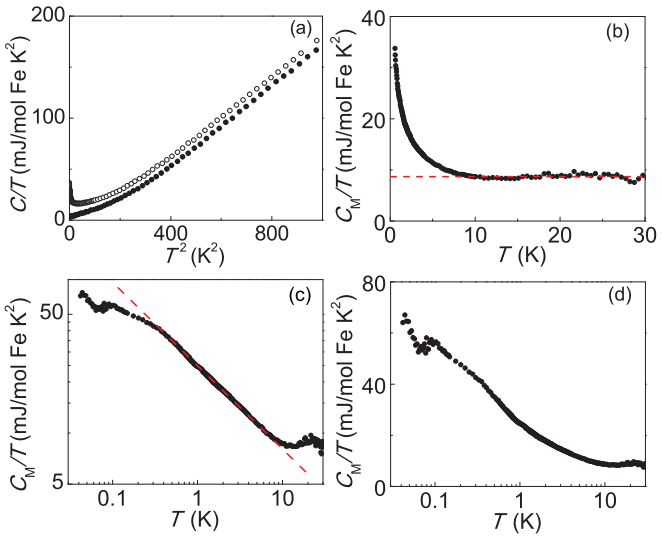


FIG. 3. (Color online) (a) As-measured specific heat $C/T$ for $YFe_2Al_{10}$ (○) and $YRu_2Al_{10}$ (●). (b) Magnetic and electronic specific heat $C_M/T$ for $YFe_2Al_{10}$. Red dashed line indicates Sommerfeld coefficient $\gamma = 9$ mJ/mol Fe K$^2$. (c) Log-log plot of $C_M/T \propto T^{-0.47}$ for $0.4\ \text{K} \leqslant T \leqslant 12$ K (red dashed line). (d) $C_M/T$ plotted as a function of $\ln T$.

## V. ELECTRICAL RESISTIVITY MEASUREMENTS

Measurements of the temperature dependence of the electrical resistivity $\rho(T)$ verify that $YFe_2Al_{10}$ is metallic. Figure 4(a) shows that $\rho(T)$ decreases from 135 $\mu\Omega$ cm at room temperature to a minimum value of $\simeq$72 $\mu\Omega$ cm near 20 K, before increasing again slightly at the lowest temperatures. This minimum resistivity in a nominally pure metal is evocative of the Kondo effect, where the measured resistivity is the sum of a Kondo impurity contribution and the background resistivity of the pristine metallic host, which here is $YFe_2Al_{10}$. We have used the measured resistivity of isoelectronic and isostructural $YbFe_2Al_{10}$ to estimate this background resistivity of $YFe_2Al_{10}$. $YbFe_2Al_{10}$ is a mixed valence system, where the Yb moments are fully compensated for $T \leqslant 400$ K. The measured $\rho(T)$ for $YbFe_2Al_{10}$ has no

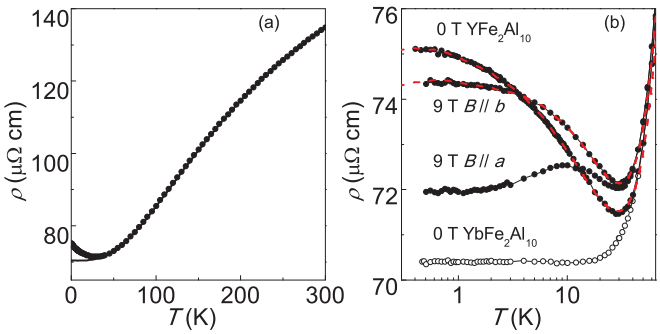


FIG. 4. (Color online) (a) As-measured electrical resistivity $\rho(T)$ for $YFe_2Al_{10}$ (●) and scaled resistivity of $YbFe_2Al_{10}$ (solid line). (b) An expanded view of the low-temperature resistive upturn from (a), comparing data for $B = 0$ with data taken with a 9 T magnetic field oriented both parallel and perpendicular to the $b$ axis (as indicated). Scaled $YbFe_2Al_{10}$ data are used to extrapolate the high-temperature $YFe_2Al_{10}$ data to $T \to 0$. Red dashed lines indicate fits to the Kondo expression described in the text.

minimum, and its magnitude can be scaled to closely resemble that of $YFe_2Al_{10}$ for 20 a$K \leqslant T \leqslant$300 K [Fig. 4(a)]. More details about $YbFe_2Al_{10}$ will be published elsewhere,[46] but its value to the present work is as a heuristic description of the resistivity of $YFe_2Al_{10}$, were the resistive upturn absent. This association provides a way to estimate the component of the total resistivity $\rho_K$ that provides the low-temperature upturn in $YFe_2Al_{10}$, where $\rho_K$ amounts to only a few percent of the total $\rho(T)$. Figure 4(b) shows that $\rho_K(T)$ displays the logarithmic increase and saturation at low temperature typical of Kondo impurities as they cross over from localized moment behavior, described by a Curie-Weiss susceptibility at high temperatures, to fully compensated moments at low temperatures, where a temperature-independent Pauli susceptibility is found. The Kondo temperature $T_K$ that sets the scale for this crossover can be determined by fitting $\rho_K(T)$ to the expression[47]

$$\rho_K = \rho_0 \left\{ 1 - \frac{\ln(T/T_K)}{\{[\ln(T/T_K)]^2 + \pi^2 S(S+1)\}^2} \right\}. \qquad (1)$$

The best fit for the $B = 0$ data has $T_K = 20 \pm 1$ K, and is compared to $\rho(T)$ in Fig. 4(b). We have investigated the effects of magnetic fields both parallel and perpendicular to the $b$ axis on $\rho(T)$. As shown in Fig. 4(b), when the field is applied along the $b$ axis, the magnitude of $\rho_K$ is decreased and moment compensation occurs below a new temperature scale $T_K = 26$ K that is larger than the zero field $T_K$, in complete agreement with the field and temperature dependence of $\rho_K$ that is found theoretically.[48] Figure 4(b) shows that there is a substantial anisotropy in $\rho_K$ when a 9 T field is applied parallel or perpendicular to the $b$ axis. This anisotropy is expected in the case of rare-earth moments, where there is a substantial electric quadrupole moment,[49] and indeed the general appearance of $\rho_K(T)$ at 9 T agrees with that reported for Ce impurities in La.[50] The chemical assay of the Y used to synthesize our samples places an upper limit of $\simeq$10 parts per million (ppm) on the rare-earth contamination level that might be responsible for $\rho_K$. Another potential source of this Kondo upturn may be site disorder or departures from stoichiometry that generate localized Fe moments. We note that single-ion anisotropy is likely to be much weaker for Fe moments in a metallic environment than for the low-lying crystal-field split levels typical of rare-earth ions. Even more important, clear evidence for the Kondo effect is generally not found for Fe concentrations larger than $\simeq$100 ppm in noble metal hosts,[51,52] where long-ranged magnetic interactions lead instead to spin-glass or long-ranged magnetic order. While we cannot be definite about the exact nature of the moments that are responsible for the Kondo upturn in the resistivity of $YFe_2Al_{10}$, we consider it likely that these moments are present only in trace amounts, at levels of 100 ppm or less, and that they originate with defects or impurities that were present in the starting materials, or were introduced during the synthesis process.

## VI. DISCUSSION

We have considered the possibility that magnetic impurities might be responsible for the $T \to 0$ divergencies in the magnetic susceptibility $\chi'$ and specific heat $C_M/T$ in $YFe_2Al_{10}$. The most prosaic example is contamination by paramagnetic impurities, however, we have demonstrated in Fig. 2(b) that the field- and temperature-dependent magnetization $M(B,T)$ does not display $B/T$ scaling and is not well described by the Brillouin function, ruling out this possibility. The resistive upturn (Fig. 4) reveals the presence of individual magnetic impurities whose moments are progressively screened by the Kondo effect below $T_K \simeq 20$ K. Disregarding the low concentration of these Kondo ions that we infer above, we note that the conventional single-channel Kondo effect does not lead to low-temperature divergencies in $C$ and $\chi'$, instead a peak is expected in $C$ for $T \simeq T_K$ and a saturation of $\chi$ for $T < T_K$. In contrast, the multichannel Kondo-effect model[53,54] does feature uncompensated moments that lead to logarithmic divergencies in both $C/T \simeq -\ln(T/T_K)$ and $\chi' \simeq -\ln(T/T_K)$. However, neither $\chi'$ [Fig. 1(c)] or $C_M/T$ [Fig. 3(d)] display these temperature dependencies.

A general argument[55,56] can be made that no single-ion model where individual magnetic moments fluctuate incoherently is consistent with the critical exponents $\gamma$ and $\beta$ found from the low-temperature magnetic susceptibility $\chi'$ and magnetization $M(B,T)/B \simeq T^{-\gamma}\mathcal{F}(B/T^{\gamma+\beta})$. Specifically, the correlation function that relates a moment $S$ at time $t$ and at $t = 0$ follows a power law $\langle S(t)S(0)\rangle \simeq 1/|t|^{2\Delta}$, where $1 - \Delta = \beta + \gamma$. We see that the requirement that the spin correlations decay with elapsed time enforces the condition that $\Delta > 0$, or equivalently that $(\beta + \gamma) < 1$ for a generic impurity model. The magnetization scaling in Fig. 2(d) gives $\beta = 0.3$ and $\gamma = 1.2$, demonstrating that this condition is violated in $YFe_2Al_{10}$. We conclude that while trace impurities or defects are presumably responsible for the resistive upturn at low temperatures, neither they nor any other isolated magnetic impurity, Kondo or otherwise, can be the source of the divergencies in the specific heat and magnetic susceptibility.

Disorder has an especially strong effect on the magnetic and electronic properties of systems that are tuned to the vicinity of a quantum critical point.[57–59] If the QCP is controlled by composition, then even small variations in composition within a sample can lead to regions that act as if they are magnetically ordered, quantum critical, or paramagnetic with differing strengths of QC fluctuations. In some cases, this leads to the formation of a cluster glass,[60–62] with strong hysteresis and frequency dependencies in measured quantities that reflect the superparamagnetic dynamics of these magnetic clusters. We have not seen these signs of cluster formation in any of our samples, and the anisotropy and field sensitivity of the magnetic susceptibility demonstrated in Fig. 1 are similarly inconsistent with such a scenario. Systems where there is a more limited range of disorder may form a Griffiths phase, where the intrinsic quantum critical response is moderated to give identical divergences in $C/T$ and in $\chi'$, i.e., $C/T \sim T^{\lambda-1}$ and $\chi' \sim T^{\lambda-1}$,[63–65] with $0 < \lambda < 1$. $\lambda$ is smallest in systems where disorder is limited and where most of the sample is nearly quantum critical, but $\lambda$ increases and the divergencies in $C$ and $\chi'$ become weaker as $\lambda$, when increasing fractions of the sample volume, are only weakly affected by the QCP. Since the temperature dependencies of $C_M/T \sim T^{-0.47}$ and $\chi' \sim T^{-1.28}$ differ significantly in $YFe_2Al_{10}$, and because the critical exponent for $\chi'$ is much larger than 1, it is unlikely that the Griffiths phase plays a significant role in this system.

TABLE I. A comparison of the temperature dependencies of the Sommerfeld coefficient $C/T$ and the uniform susceptibility $\chi(T)$ for $YFe_2Al_{10}$, as well as theoretical results for different quantum critical antiferromagnets and ferromagnets.

| | $C/T$ | $\chi(T)$ | Reference |
|---|---|---|---|
| $YFe_2Al_{10}$ | $T^{-0.47}$ | $T^{-1.28}$ | This work |
| 3D Ising | | $T^{-1.237}$ | 66 |
| 3D Heisenberg | | $T^{-1.387}$ | 66 |
| Mean field | | $T^{-1}$ | |
| 3D clean FM | | $T^{-1}$ | 37 |
| 2D AF | $\ln(T^*/T)$ | $\chi_0 - aT$ | 67 and 68 |
| 2D clean FM | $T^{-1/3}$ | $T^{-1}$ | 24 |
| 2D dirty FM | $T^{-1/2}$ | $T^{-1}$ | 24 |
| 3D AF | $\gamma_0 - a\sqrt{T}$ | $T^{-3/2}$ | 24,69 and 70 |
| 3D clean FM | $\ln(T^*/T)$ | $T^{-4/3}$ | 24 and 69 |
| 3D dirty FM | $T^{-1/4}$ | $T^{-5/4}$ | 24 and 69 |

The general failure of single-ion and disorder models to describe the temperature divergencies of the specific heat and magnetic susceptibility implies that the underlying quantum criticality in $YFe_2Al_{10}$ results from proximity to a bulk phase transition that occurs at $T = 0$. Since no long-ranged magnetic order is observed in $YFe_2Al_{10}$, there is no way to determine *a priori* whether the QCP is ferromagnetic or antiferromagnetic, and we consider both possibilities in our analysis of the critical exponents. The temperature divergencies of the specific heat $C_M/T \sim T^{-0.47}$ and the uniform $B \to 0$ ac susceptibility $\chi' \sim T^{-\gamma}$ ($\gamma = 1.28 \pm 0.04$) are compared in Table I to theoretical results derived for both antiferromagnetic and ferromagnetic phase transitions. The susceptibility exponent $\gamma = 1.28 \pm 0.04$ is in reasonable agreement with classical Ising or Heisenberg exponents but not with the mean-field value.[66] Since the critical behavior extends to very low temperatures, if not to $T = 0$, it is expected that the classical models will be replaced with their quantum critical analogs. However, the susceptibility divergence in $YFe_2Al_{10}$ is much too strong to be consistent with field theory results for the three-dimensional quantum critical ferromagnet[37] or with experimental results that find $\gamma \to 0$ near a ferromagnetic QCP.[45]

Spin-fluctuation theories provide a complete set of exponents for both $C_M/T$ and $\chi'(T)$, in both ferromagnets and antiferromagnets, and in two and three dimensions.[24,67] Given the strong low-temperature anisotropy in $\chi'$, we allow for the possibility that the critical magnetic fluctuations could be quasi-two-dimensional, or fully three dimensional. On first inspection of Table I, there does not seem to be a single model that simultaneously describes the temperature divergencies of both the specific heat and the magnetic susceptibility in $YFe_2Al_{10}$. The temperature dependence of $\chi'$ is in good agreement with those expected for clean and dirty three-dimensional ferromagnets, but the corresponding specific-heat temperature dependencies are not consistent with the observed power-law divergence of $C_M/T$. Conversely, the observed temperature dependence of the specific heat suggests that the nearby QCP is that of a two-dimensional dirty ferromagnet; the observed susceptibility diverges more strongly than this model predicts. It is worth emphasizing that the results in Table I extend only to the quantum critical contributions to the magnetic susceptibility and specific heat, and that the measured $C$ and $\chi'$ may include other temperature-dependent contributions as well. The specific heat is thought to be particularly problematic,[34] since it is also sensitive to variations in the electronic density of states, which may be strongly modified in the vicinity of the QCP. Similarly, we point out that the measured uniform susceptibility is not necessarily the true critical susceptibility, which for an antiferromagnet must be measured at the antiferromagnetic wave vector using neutron scattering. Further, a complex magnetic structure may involve both ferromagnetic and antiferromagnetic components that both contribute to the temperature-dependent susceptibility, although ultimately only one is likely to be quantum critical. Finally, we note that the temperature dependencies in Table I represent the classical regime associated with a $T = 0$ phase transition, since this is the regime most likely to be experimentally accessed. It is possible that the temperature dependencies that are observed in our experiments correspond to crossover behaviors that connect the classical and quantum regimes near a $T \to 0$ phase transition,[67] from two-dimensional quantum criticality at higher temperatures to fully three-dimensional criticality at lower temperatures,[71] or alternatively from the quantum critical to Fermi-liquid regimes,[70] depending on whether the composition of $YFe_2Al_{10}$ locates it on the ordered (but with $T_N \leqslant 0.09$ K) or Fermi-liquid (but with $T_{FL} \leqslant 0.4$ K) sides of the implied QCP. Experiments that use compositional variations to drive $YFe_2Al_{10}$ through the QCP into the ordered phase would be most useful for resolving the apparent disagreement between the critical behaviors of the specific heat and magnetic susceptibility.

## VII. CONCLUSION

The experimental information that we report here indicates that $YFe_2Al_{10}$ is a system that is very close to a QCP, and no magnetic order is found for temperatures larger than 0.09 K. The critical fluctuations associated with this $T = 0$ phase transition dominate the specific heat $C_M/T$ and ac susceptibility $\chi'$, and both display power-law temperature divergencies at the lowest temperatures. $\chi'$ is strongly anisotropic, and only diverges when the ac field is in the ac plane, suggesting that these critical fluctuations are quasi-two-dimensional. Magnetic fields suppress these fluctuations, and field-temperature scaling is found for fields as large as 7 T. It is also possible that a magnetic field may also serve as a tuning parameter, driving the system away from the QCP that dominates $YFe_2Al_{10}$ for $B = 0$. The critical exponents found for $C_M/T$ and $\chi'$ are not simultaneously explained by existing spin fluctuation, Hertz-Millis, or field-theoretical results. However, the strength of the divergence in $\chi'(T)$ and the nonlogarithmic divergence in $C_M/T$ are inconsistent with single impurity or known disorder models, indicating that the implied QCP is intrinsic and representative of bulk, stoichiometric $YFe_2Al_{10}$. $YFe_2Al_{10}$ serves as a valuable bridge between studies of quantum criticality in $f$-electron systems that span magnetic order to QCP to strongly interacting Fermi liquid, and the stoichiometric $d$-electron systems where magnetic order—indeed, mostly ferromagnetic order—must be tuned to instability using pressure, composition, or magnetic

fields. Since $YFe_2Al_{10}$ is naturally located near a QCP, but is apparently not ordered, it holds out the possibility of a complete investigation of the QC behavior using probes such as neutron scattering, thermal expansion, and thermal measurements such as specific heat that are difficult or impossible to implement when pressure is used as a tuning parameter, but without incurring the complications of the disorder that invariably accompany chemical doping experiments.

## ACKNOWLEDGMENTS

This work was carried out under the auspices of the US Department of Energy, Office of Basic Energy Sciences under Contract No. DE-AC02-98CH1886. The authors thank A. Tsvelik, C. Geibel, T. Takabatake, M. Baenitz, M. Brando, and A. Strydom for interesting discussions, and P. Khalifah for assistance with x-ray-diffraction measurements.

*maronson@bnl.gov

[1] C. M. Varma, P. B. Littlewood, S. Schmitt-Rink, E. Abrahams, and A. E. Ruckenstein, Phys. Rev. Lett. **63**, 1996 (1989).
[2] R. B. Laughlin, Adv. Phys. **47**, 943 (1998).
[3] D. M. Broun, Nat. Phys. **4**, 170 (2008).
[4] J. Dai, Q. Si, J.-X. Zhu, and E. Abrahams, Proc. Natl. Acad. Sci. USA **106**, 4118 (2009).
[5] G. R. Stewart, Rev. Mod. Phys. **73**, 797 (2001).
[6] H. v. Lohneysen, A. Rosch, M. Vojta, and P. Wölfle, Rev. Mod. Phys. **79**, 1015 (2007).
[7] P. Gegenwart, Q. Si, and F. Steglich, Nat. Phys. **4**, 186 (2008).
[8] D. Jaccard, H. Wilhelm, D. Jérome, J. Moser, C. Carcel, and J. M. Fabre, J. Phys.: Condens. Matter **13**, L89 (2001).
[9] S. M. Hayden, G. Aeppli, H. Mook, D. Rytz, M. F. Hundley, and Z. Fisk, Phys. Rev. Lett. **66**, 821 (1991).
[10] M. C. Aronson, R. Osborn, R. A. Robinson, J. W. Lynn, R. Chau, C. L. Seaman, and M. B. Maple, Phys. Rev. Lett. **75**, 725 (1995).
[11] A. Schroder, G. Aeppli, R. Coldea, M. Adams, O. Stockert, H. v. Löhneysen, E. Bucher, R. Ramazashvili, and P. Coleman, Nature (London) **407**, 351 (2000).
[12] Q. Si, S. Rabello, K. Ingersent, and J. L. Smith, Nature (London) **413**, 804 (2001).
[13] P. Coleman and A. J. Schofield, Nature (London) **433**, 226 (2005).
[14] N. D. Mathur, F. M. Grosche, S. R. Julian, I. R. Walker, D. M. Freye, R. K. W. Haselwimmer, and G. G. Lonzarich, Nature (London) **394**, 39 (1998).
[15] S. S. Saxena, P. Agarwal, K. Ahilan, F. M. Grosche, R. K. W. Haselwimmer, M. J. Steiner, E. Pugh, I. R. Walker, S. R. Julian, P. Monthoux, G. G. Lonzarich, A. Huxley, I. Sheikin, D. Braithwaite, and J. Flouquet, Nature (London) **406**, 587 (2000).
[16] R. A. Borzi, S. A. Grigera, J. Farrell, R. S. Perry, S. J. S. Lister, S. L. Lee, D. A. Tennant, Y. Maeno, and A. P. Mackenzie, Science **315**, 214 (2007).
[17] C. Pfleiderer, A. Neubauer, S. Muhlbauer, F. Jonietz, M. Janoschek, S. Legl, R. Ritz, W. Munzer, C. Franz, P. G. Niklowitz, T. Keller, R. Georgii, P. Boni, B. Binz, A. Rosch, U. K. Rossler, and A. N. Bogdanov, J. Phys. Condens.: Matter **21**, 164215 (2009).
[18] P. C. Coleman, Phys. Status Solidi **247**, 506 (2010)
[19] S. Paschen, T. Lührmann, S. Wirth, P. Gegenwart, O. Trovarelli, C. Geibel, F. Steglich, P. Coleman, and Q. Si, Nature (London) **432**, 881 (2004).
[20] H. Shishido, R. Settai, H. Harima, and Y. Onuki, J. Phys. Soc. Jpn. **74**, 1103 (2005).
[21] S. L. Bud'ko, E. Morosan, and P. C. Canfield, Phys. Rev. B **71**, 054408 (2005).
[22] P. Gegenwart, T. Westerkamp, C. Krellner, Y. Tokiwa, S. Paschen, C. Geibel, F. Steglich, E. Abrahams, and Q. Si, Science **315**, 969 (2007).
[23] S. Friedemann, T. Westerkamp, M. Brando, N. Oeschler, S. Wirth, P. Gegenwart, C. Krellner, C. Geibel, and F. Steglich, Nat. Phys. **5**, 465 (2009).
[24] C. Pfleiderer, G. J. McMullan, S. R. Julian, and G. G. Lonzarich, Phys. Rev. B **55**, 8330 (1997).
[25] S. A. Grigera, R. S. Perry, A. J. Schofield, M. Chiao, S. R. Julian, G. G. Lonzarich, S. I. Ikeda, Y. Maeno, A. J. Millis, and A. P. Mackenzie, Science **294**, 329 (2001).
[26] M. Uhlarz, C. Pfleiderer, and S. M. Hayden, Phys. Rev. Lett. **93**, 256404 (2004).
[27] D. A. Sokolov, M. C. Aronson, W. Gannon, and Z. Fisk, Phys. Rev. Lett. **96**, 116404 (2006).
[28] D. Moroni-Klementowicz, M. Brando, C. Albrecht, W. J. Duncan, F. M. Grosche, D. Gruner, and G. Kreiner, Phys. Rev. B **79**, 224410 (2009).
[29] G. G. Lonzarich and L. Taillefer, J. Phys. C **18**, 4339 (1985).
[30] R. Viennois, S. Charar, D. Ravot, P. Haen, and A. Mauger, Eur. Phys. J. B **46**, 257 (2005).
[31] S. Jia, S. L. Bud'ko, G. D. Samolyuk, and P. C. Canfield, Nat. Phys. **3**, 334 (2007).
[32] M. Brando, W. J. Duncan, D. Moroni-Klementowicz, C. Albrecht, D. Grüner, R. Ballou, and F. M. Grosche, Phys. Rev. Lett. **101**, 026401 (2008).
[33] W. J. Duncan, O. P. Welzel, D. Moroni-Klementowicz, C. Albrecht, P. G. Niklowitz, D. Gruner, M. Brando, A. Neubauer, C. Pfleiderer, N. Kikugawa, A. P. Mackenzie, and F. M. Grosche, Phys. Status Solidi B **247**, 544 (2010).
[34] A. W. Rost, A. M. Berridge, R. S. Perry, J.-F. Mercure, S. A. Grigera, and A. P. Mackenzie, Phys. Status Solidi B **247**, 513 (2010).
[35] T. Waki, S. Terazawa, Y. Tabata, F. Oba, C. Michioka, K. Yoshimura, S. Ikeda, H. Kobayashi, K. Ohoyama, and H. Nakamura, J. Phys. Soc. Jpn. **79**, 043701 (2010).
[36] M. Nicklas, M. Brando, G. Knebel, F. Mayr, W. Trinkl, and A. Loidl, Phys. Rev. Lett. **82**, 4268 (1999).
[37] D. Belitz, T. R. Kirkpatrick, and T. Vojta, Rev. Mod. Phys. **77**, 579 (2005).
[38] N. Morozov, L. Krusin-Elbaum, T. Shibauchi, L. N. Bulaevskii, M. P. Maley, Yu. I. Latyshev, and T. Yamashita, Phys. Rev. Lett. **84**, 1784 (2000).
[39] V. M. T. Thiede, T. Ebel, and W. Jeitschko, J. Mater. Chem. **8**, 125 (1998).
[40] A. M. Strydom and P. Peratheepan, Phys. Status Solidi **4**, 356 (2010).
[41] L. J. Farrugia, J. Appl. Crystallogr. **32**, 837 (1999).
[42] J. C. Waerenborgh, P. Salamakha, O. Sologub, S. Serio, M. Godinho, A. P. Goncalves, and M. Almeida, J. Alloys Compd. **323-324**, 78 (2001).

[43] J. Custers, P. Gegenwart, H. Wilhelm, K. Neumaier, Y. Tokiwa, O. Trovarelli, C. Geibel, F. Steglich, C. Pépin, and P. Coleman, Nature (London) **424**, 524 (2003).
[44] A. Bianchi, R. Movshovich, I.Vekhter, P. G. Pagliuso, and J. L. Sarrao, Phys. Rev. Lett. **91**, 257001 (2003).
[45] N. P. Butch and M. B. Maple, Phys. Rev. Lett. **103**, 076404 (2009).
[46] L. S. Wu, M. S. Kim, and M. C. Aronson (unpublished).
[47] D. R. Hamann, Phys. Rev. **158**, 570 (1967).
[48] P. Schlottmann, Phys. Rev. B **35**, 5279 (1987).
[49] A. Fert, J. Phys. F **3**, 2126 (1973).
[50] K. Samwer and K. Winzer, Z. Phys. B **25**, 269 (1976).
[51] J. W. Loram, T. E. Whall, and P. J. Ford, Phys. Rev. B **2**, 857 (1976).
[52] D. Riegel, L. Büermann, K. D. Gross, M. Luszik-Bhadra, and S. N. Mishra, Phys. Rev. Lett. **62**, 316 (1989).
[53] D. L. Cox and M. Jarrell, J. Phys.: Condens. Matter **8**, 9825 (1996).
[54] H. Amitsuka and T. Sakakibara, J. Phys. Soc. Jpn. **63**, 736 (1994).
[55] B. Andraka and A. M. Tsvelik, Phys. Rev. Lett. **67**, 2886 (1991).
[56] A. M. Tsvelik and M. Reizer, Phys. Rev. B **48**, 9887 (1993).
[57] A. Rosch, Phys. Rev. Lett. **82**, 4280 (1999).
[58] T. Vojta, J. Phys. A **39**, R143 (2006).
[59] T. Vojta, J. Low Temp. Phys. **161**, 299 (2010).
[60] T. Westerkamp, M. Deppe, R. Küchler, M. Brando, C. Geibel, P. Gegenwart, A. P. Pikul, and F. Steglich, Phys. Rev. Lett. **102**, 206404 (2009).
[61] I. Tamura, T. Mizushima, Y. Isikawa, and J. Sakurai, J. Magn. Magn. Mater. **20**, 31 (2000).
[62] M. Kolenda, M. D. Koterlin, M. Hofmann, B. Penc, A. Szytuła, A. Zygmunt, and J. Zukrowski, J. Alloys Compd. **327**, 21 (2001).
[63] A. H. Castro Neto and B. A. Jones, Phys. Rev. B **62**, 14975 (2000).
[64] A. J. Millis, D. K. Morr, and J. Schmalian, Phys. Rev. **66**, 174433 (2002).
[65] S. Ubaid-Kassis, T. Vojta, and A. Schroeder, Phys. Rev. Lett. **104**, 066402 (2010).
[66] J. C. Le Guillou and J. Zinn-Justin, Phys. Rev. Lett. **39**, 95 (1977).
[67] A. J. Millis, Phys. Rev. B **48**, 7183 (1993).
[68] L. B. Ioffe and A. J. Millis, Phys. Rev. B **51**, 16151 (1995).
[69] U. Zülicke and A. J. Millis, Phys. Rev. B **51**, 8996 (1995).
[70] T. Moriya and T. Takimoto, J. Phys. Soc. Jpn. **64**, 960 (1995).
[71] M. Garst, L. Fritz, A. Rosch, and M. Vojta, Phys. Rev. B **78**, 235118 (2008).